

Large-scale coherent rotation and oscillation in turbulent thermal convection

X.-L. Qiu, S. H. Yao, and P. Tong*

Department of Physics, Oklahoma State University, Stillwater, Oklahoma 74078

(Received 6 April 2000)

Laser Doppler velocimetry is used to measure the velocity profile of turbulent thermal convection in an aspect-ratio-one cell filled with water. Velocity fluctuations are found to be homogeneous and isotropic in the turbulent bulk region. Despite the large velocity fluctuations, the mean flow field maintains a large-scale structure, which rotates and oscillates in a coherent manner. The experiment suggests a unique driving mechanism for the large-scale coherent rotation and oscillation in turbulent convection.

PACS number(s): 47.27.-i, 47.27.Te, 44.25.+f

Turbulent thermal convection is an intriguing problem in nonlinear physics and has attracted much attention in recent years [1]. Despite its special way of generating turbulence at large length scales and its relatively low Reynolds number (Re), turbulent convection shares many common features that are usually associated with high- Re turbulent flows. These features include coherent structures, intermittent fluctuations, and anomalous scaling. Over the past decade, many temperature and heat transport measurements have been carried out in turbulent convection under various experimental conditions [2]. These measurements find scaling laws in the heat flux and temperature statistics and have stimulated considerable theoretical efforts [3–5], aimed at explaining the observed scaling laws. Like many transport phenomena in condensed matter physics, however, the measured macroscopic transport properties can often be explained by theories with different microscopic mechanisms. The theoretical calculations arrive at similar conclusions for the temperature field but have different assumptions and predictions for the velocity field. Direct measurements of the large-scale flow structure, therefore, become important to verify assumptions and test predictions of the theoretical models [3–5].

A main issue of an unresolved theoretical debate is to understand whether the heat transport in turbulent convection is determined primarily by the thermal plumes that erupt from the upper and lower boundary layers or by the large-scale circulation that spans the height of the cell. These two coherent structures are found to coexist in the convection cell by flow visualization, but quantitative information about their structure, dynamics, and interaction is limited. While the recent local velocity measurements [6,7] at the cell center and near the boundary are useful in determining the scaling relations of the velocity fluctuation at a few specific positions in the cell, the overall flow structure of turbulent convection has remained elusive. The lack of the velocity information prevents us from answering some important questions that are related directly to the physical understanding of convective turbulence in general. These questions include: How is the large-scale circulation generated and sustained? At what length scale and how does temperature become a passive scalar? What is the connection between the thermal plumes and the large-scale circulation?

In this Rapid Communication, we report laser Doppler velocimetry (LDV) measurements of the velocity profile in an aspect-ratio-one cell filled with water. LDV measures the local velocity as a function of time and the velocity profile is obtained by scanning the velocity probe over the whole convection cell. As will be shown below, because of the spatial confinement, the large-scale motion in turbulent convection is stabilized in the closed cell and thus LDV can be used to study its dynamics in great detail. It is found that LDV is capable of measuring the local velocity with high accuracy (better than 1%) over the entire cell, except near the upper and lower thermal boundary layers whose thickness is of the order of 1 mm. In the boundary layer region, fluctuations of the fluid refractive index due to large temperature fluctuations cause the two laser beams used in LDV to wander and defocus in the fluid. This corruption of laser beam properties reduces the signal-to-noise level of LDV.

The experiment was conducted in a cylindrical cell with an inner diameter of $D = 19$ cm and height $L = 20.4$ cm. Details about the apparatus have been described elsewhere [7], and here we mention only some key points. The upper and lower plates were made of brass and the sidewall was a cylindrical ring made of transparent Plexiglas with a long rectangular flat window for the velocity measurement. The temperature of the upper plate was regulated by passing cold water through a cooling chamber fitted on the top of the plate. The lower plate was heated uniformly with an electric film heater. The control parameter was the Rayleigh number Ra , which is proportional to L^3 and to the temperature difference ΔT between the two plates. In the experiment, the bulk fluid temperature was kept at 30°C and the corresponding Prandtl number was 5.4. The velocity measurements were carried out using a commercial LDV (TSI Inc.) together with an argon ion laser. A typical sampling rate was 10–15 Hz, which is ~ 10 times higher than the cutoff frequency in the velocity power spectrum.

Figure 1(a) shows the measured mean velocity $v(z)$ and its standard deviation $\sigma(z)$ as a function of the normalized vertical distance z/L away from the center of the bottom plate. Each data point was averaged over 2 h and the measurements were made at $Ra = 3.7 \times 10^9$. It is seen that the flow field can be divided into three different regions:

(I) In the thin viscous boundary layer ($z/L \leq 0.04$), the horizontal mean velocity $v_h(z)$ (open circles) and its variance $\sigma_h(z)$ (open squares) both increase linearly with z and

*Email address: ptong@okstate.edu

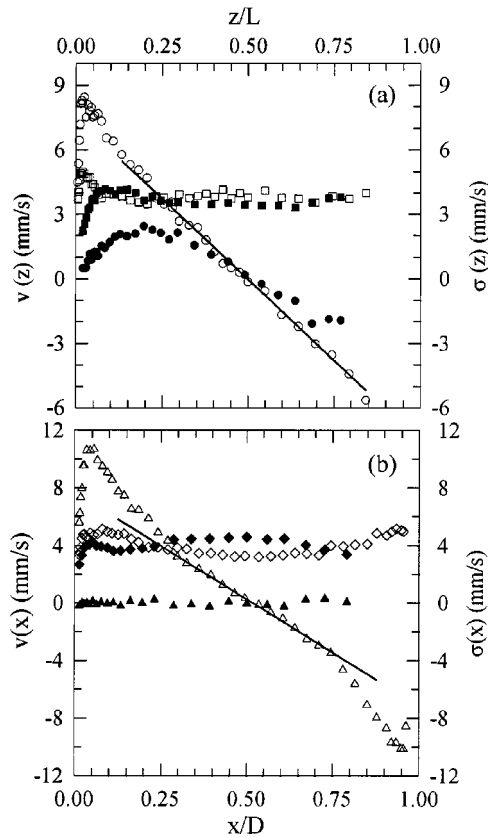


FIG. 1. (a) Measured mean velocity profiles (circles) and rms profiles (squares) as a function of z/L . The open symbols represent the velocity component in the horizontal direction, and the closed symbols are in the vertical direction. (b) Measured mean velocity profiles (triangles) and rms profiles (diamonds) as a function of x/D . The open symbols represent the velocity component along the large-scale rotation, and the closed symbols are in the direction perpendicular to the rotation plane. The solid lines are the linear fits to the mean velocity profiles.

then reach a maximum value at $z/L \approx 0.04$. At this position, $v_h(z)$ is ~ 1.6 times larger than $\sigma_h(z)$. The vertical mean velocity $v_v(z)$ (closed circles), however, increases with z much more slowly and its value at $z/L \approx 0.04$ is only $1/8$ of $v_h(z)$. The vertical velocity fluctuations are found to be always larger than their mean values. Clearly, $v_h(z)$ is the dominant velocity component in the boundary region. The fact that $\sigma_h(z)$ peaks at $z/L \approx 0.04$ indicates that velocity fluctuations are generated mainly in the boundary region.

(II) It is also seen from Fig. 1(a) that $\sigma_h(z)$ becomes larger than $v_h(z)$ when $0.75 > z/L > 0.25$. Velocity fluctuations in the central region are homogeneous and nearly isotropic. Despite the large velocity fluctuations, the mean flow field maintains a coherent structure. The measured $v_h(z)$ is well fitted by a linear function (solid line), suggesting that the bulk fluid undergoes a coherent rotation around the cell center. From the flow visualization we find that the large-scale coherent rotation (LSCR) is not exactly of circular shape; rather, it rotates around an ellipse whose long axis is tilted at an angle with respect to the vertical direction. Because of this tilt, the measured mean velocity has a smaller vertical component $v_v(z)$, which can also be fitted to a linear function. From the ratio of the two slopes, we find the tilt angle $\alpha \approx 33.5^\circ$.

(III) The intermediate region between the viscous boundary layer and the central core region is the buffer layer ($0.04 < z/L \leq 0.25$), which was also called the mixing zone [3]. Velocity fluctuations in this region remain approximately the same as those in the central region. Their variance is small when compared with $v_h(z)$ but is larger than $v_v(z)$. Because of the eruptive nature of the thermal plumes, their rising velocity should be comparable to σ_v , which can be estimated by balancing the buoyancy with the viscous drag. Using the mixing length theory [8], we find $\sigma_v \approx 4.4$ mm/s, which is very close to the measured value $\sigma_v \approx 4$ mm/s at $z/L \approx 0.04$.

We also measured the mean velocity $v(x)$ and its standard deviation $\sigma(x)$ as a function of the normalized horizontal distance x/D away from the sidewall in the horizontal midplane of the cell. It is seen from Fig. 1(b) that the velocity profile near the sidewall (open triangles) can also be described by three subregions similar to those shown in Fig. 1(a). In the central region, the mean velocity profiles along the x axis and the z axis overlap, suggesting that the bulk fluid indeed undergoes a coherent rotation. The measured $v(x)$ peaks at $x/D \approx 0.05$ and its maximum value is 25% larger than $v_h(z)$ at $z/L \approx 0.04$. It is also seen that the mean velocity in the direction perpendicular to the rotation plane (closed triangles) is close to zero but its variance (closed diamonds) is approximately the same as those in the other two directions. Figure 1 thus demonstrates that turbulent convection in the aspect-ratio-one cell has a stable, quasi-two-dimensional flow structure. Measurements of the velocity profile at other Rayleigh numbers ($10^9 \leq Ra \leq 10^{10}$) confirm that the flow structure in turbulent convection remains invariant for different Ra .

From the flow visualization we have observed that the thermal plumes emitted from the upper and lower surfaces are often sheared to the sidewall region by the large-scale horizontal flow near the boundary. As a result, warm fluids rise along one side of the cell and cold fluids fall on the opposite side of the cell. Regions occupied by the warm and cold plumes coincide with the “buffer layers” near the sidewall, in which the local velocity reaches maximum. The fact that the maximum velocity near the sidewall is larger than that near the upper and lower surfaces suggests that the LSCR is driven by the rising and falling plumes near the sidewall. The central core region is “sheared” by the vertical flow in the plume-dominated regions and remains passive with a constant mean velocity gradient.

From the above velocity measurements together with the flow visualization, we arrive at the following driving mechanism for the LSCR. The outer region of the rotation (i.e., the “buffer layers” around the cell boundary) is the active region that drives the LSCR. Thermal plumes erupt into the region from the upper and lower thermal boundary layers and many of them are sheared to the sidewall region by the large-scale horizontal flow near the boundary. The warm and cold plumes separated laterally in the two opposing sidewall regions exert buoyancy forces on the bulk fluid and drive the vertical flow near the sidewall. This vertical flow near the sidewall in turn enhances the horizontal flow near the upper and lower surfaces. This is a self-feeding process, which connects the thermal plumes with the LSCR. The central

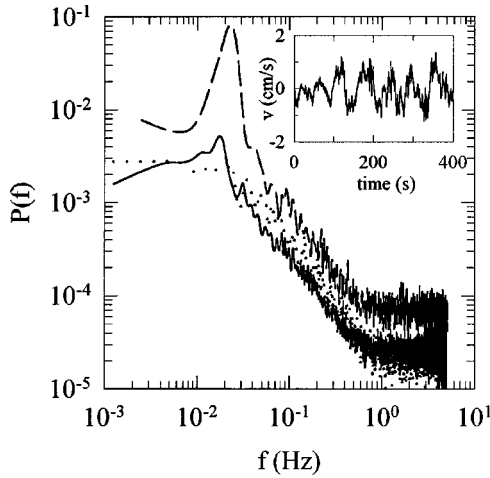


FIG. 2. Measured frequency power spectra $P(f)$ for the horizontal (solid curve) and vertical (dotted curve) velocity components in the rotation plane and for the velocity component perpendicular to the rotation plane (dashed curve). The inset shows the time series data corresponding to the dashed curve. The measurements were conducted at the cell center with $Ra=3.7 \times 10^9$.

core region is a passive region, which is “sheared” by the outer region of the rotation. The velocity fluctuations in the central region are homogeneous and isotropic, and they are strong enough to fully mix all the energetic thermal plumes penetrated into the region. Early temperature measurements [9] have shown that the azimuth of the LSCR rotates slowly in time when the cylindrical cell is leveled perfectly. To pin down the azimuthal rotation, we tilted the cell by a small angle ($<1^\circ$) in the above velocity measurements. Ciliberto *et al.* [10] have shown that such a small tilt does not affect turbulent convection very much.

Besides their spatial separation, the thermal plumes emitted from the upper and lower surfaces are also coupled in time. Figure 2 shows the frequency power spectra $P(f)$ for three orthogonal velocity components at the cell center. The power spectra were obtained using a fast Fourier transform (FFT) program provided by TSI. In the FFT, we used 4096 data points and the result was averaged over 7 h. It is seen that the measured $P(f)$ for the two horizontal velocity components has a sharp peak at $f_0 \approx 0.02$ Hz, whereas the measured $P(f)$ for the vertical velocity does not show any prominent peak. Figure 2 thus demonstrates that the velocity field has a well-defined oscillation in the horizontal direction. In fact, this horizontal oscillation can be observed directly from the time series data (see the inset). We also measured $P(f)$ at other locations and find that the measured $P(f)$ for the two horizontal velocity components at different values of z peaks at the same frequency f_0 , and the amplitude of the peak remains approximately the same as z/L is varied from 0.04 to 0.5. These measurements reveal that the horizontal oscillation is not confined at the cell center but is associated with the large-scale motion of the bulk fluid.

To find the origin of the oscillation, we measure the Ra -dependence of the oscillation frequency $\omega_h = 2\pi f_0$ and compare it with the rotational frequency γ_h of the LSCR. The value of γ_h is obtained from the slope of the linear horizontal velocity profile shown in Fig. 1(a). Figure 3 compares the normalized oscillation frequency $\omega_h L^2/\kappa$ (open circles) with

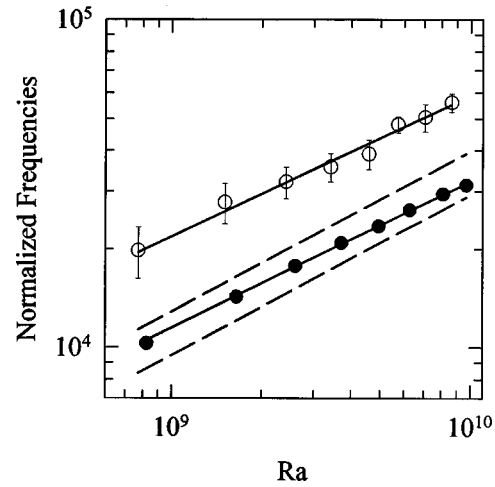


FIG. 3. Normalized oscillation frequency $\omega_h L^2/\kappa$ (open circles) and rotational frequency $\gamma_h L^2/\kappa$ (closed circles) as a function of Ra . The solid lines are the power-law fits to the data. The dashed lines show the normalized temperature frequency $\omega_p L^2/\kappa$ obtained by Castaing *et al.* [3] (lower dashed line) and by Cioni *et al.* [9] (upper dashed line).

the rotational frequency $\gamma_h L^2/\kappa$ (closed circles) for different values of Ra . The measured $\omega_h L^2/\kappa$ can be well described by a power law $\omega_h L^2/\kappa = 2.9 Ra^\epsilon$ (upper solid line) with the exponent $\epsilon = 0.43 \pm 0.06$. The lower solid line shows the power law fit $\gamma_h L^2/\kappa = 1.1 Ra^{0.45}$. Within the experimental uncertainties, the two power laws have essentially the same exponent close to $3/7$ but their amplitudes differ by a factor of 1.85.

The emergence of a sharp peak in the velocity power spectrum is an intriguing feature of turbulent convection. It has been shown previously that the temperature power spectrum also has a peak at low frequency [3]. This temperature oscillation was found in the regions near the upper and lower boundary layers and its frequency ω_p has been linked to the rotational frequency of the large-scale circulation [11]. The dashed lines in Fig. 3 show the normalized temperature frequency $\omega_p L^2/\kappa$ obtained in low temperature helium gas (lower dashed line: $\omega_p L^2/\kappa = 0.36 Ra^{0.491}$) [3] and in water (upper dashed line: $\omega_p L^2/\kappa \approx 0.5 Ra^{0.49}$) [9]. Indeed, the measured temperature frequencies in the two systems are close to the rotational frequency γ_h [12].

Recently, Villermaux [13] proposed a dynamic model to explain the observed temperature oscillation. The model assumes that the unstable modes in the upper and lower thermal boundary layers interact through a delayed nonlinear coupling with a time constant $\tau \approx (2\gamma_h)^{-1}$. Because of this delayed coupling, the unstable modes (i.e., the thermal plumes) are excited alternately between the upper and lower boundary layers with a local frequency $\omega_p \approx \gamma_h$. While Villermaux’s model explained the emission dynamics of the thermal plumes, it did not discuss the dynamic consequences of the alternating plume emission to the flow field. With the above velocity measurements together with the flow visualization, we now can provide a complete physical picture to link the local plume emission to the global flow structure. Because of the buoyancy acceleration, the thermal plumes exert vertical forces on the bulk fluid. An alternating eruption of the thermal plumes, therefore, will give rise to a pe-

riodic impulsive force to the fluid. As discussed above, the thermal plumes emitted from the upper and lower surfaces are often sheared to the two opposing sidewall regions by the large-scale horizontal flow. Because of the spatial separation of the warm and cold plumes, the vertical thermal forcing results in a periodic impulsive torque in the plume-dominated sidewall region. It is this periodic torque that drives the LSCR continuously. Because the thermal forcing is of long-range, the velocity oscillation is found in the bulk region of the flow.

We believe that the velocity oscillation observed in the aspect-ratio-one cell is the response of the bulk fluid to the horizontal perturbations produced by the warm and cold plumes near the sidewall. During the eruption period, the rising (and falling) plumes can produce a time-dependent

horizontal disturbance to the (tilted) coherent rotation in the central region of the cell. From the velocity measurements in other cells, we find that the velocity oscillation is sensitive to the aspect ratio of the convection cell [14]. A theoretical model is needed to further explore the detailed dynamics of the velocity oscillation. Clearly, the present experiment provides an interesting example to demonstrate how otherwise random unstable modes in a closed system are organized in both space and time to generate a large-scale flow structure, which rotates and oscillates coherently in a turbulent environment.

We thank M. Lucas and his team for fabricating the convection cell. This work was supported by the National Science Foundation under Grant No. DMR-9623612.

-
- [1] E. Siggia, *Annu. Rev. Fluid Mech.* **26**, 137 (1994).
 [2] F. Heslot *et al.*, *Phys. Rev. A* **36**, 5870 (1987); T. H. Solomon and J. P. Gollub, *Phys. Rev. Lett.* **64**, 2382 (1990); A. Belmonte *et al.*, *Phys. Rev. E* **50**, 269 (1995); Y.-M. Liu and R. E. Ecke, *Phys. Rev. Lett.* **79**, 2257 (1997); J. A. Glazier *et al.*, *Nature (London)* **398**, 307 (1999).
 [3] B. Castaing *et al.*, *J. Fluid Mech.* **204**, 1 (1989).
 [4] B. I. Shraiman and E. D. Siggia, *Phys. Rev. A* **42**, 3650 (1990).
 [5] S. Grossmann and D. Lohse, *J. Fluid Mech.* **407**, 27 (2000).
 [6] A. Tilgner, A. Belmonte, and A. Libchaber, *Phys. Rev. E* **47**, R2253 (1993).
 [7] Y. Shen, K.-Q. Xia, and P. Tong, *Phys. Rev. Lett.* **75**, 437 (1995); Y.-B. Xin, K.-Q. Xia, and P. Tong, *ibid.* **77**, 1266 (1996).
 [8] R. H. Kraichnan, *Phys. Fluids* **5**, 1374 (1962).
 [9] S. Cioni, S. Ciliberto, and J. Sommeria, *J. Fluid Mech.* **335**, 111 (1997).
 [10] S. Ciliberto, S. Cioni, and C. Laroche, *Phys. Rev. E* **54**, R5901 (1996).
 [11] M. Sano, X.-Z. Wu, and A. Libchaber, *Phys. Rev. A* **40**, 6421 (1989).
 [12] The small differences between ω_p and γ_h may be related to the fact that ω_p is measured near the boundary and thus is connected to the maximum velocity at $z/L \approx 0.04$, whereas γ_h is obtained from the velocity profile in the central region of the cell.
 [13] E. Villiermaux, *Phys. Rev. Lett.* **75**, 4618 (1995).
 [14] X.-L. Qiu *et al.* (unpublished).